

# Mössbauer Study and Nonlinear Excitations in the Antiferromagnetic Chain of $\text{Rb}_2\text{Mn}_{1-x}\text{Fe}_x\text{F}_5\cdot\text{H}_2\text{O}$ ( $x \leq 0.50$ )<sup>†</sup>

Jürgen Pebler

Received October 14, 1987

Mössbauer-effect measurements have been performed on the quasi-1-D antiferromagnetic solid solutions of  $\text{Rb}_2\text{Mn}_{1-x}\text{Fe}_x\text{F}_5\cdot\text{H}_2\text{O}$  ( $x \leq 0.50$ ) as a function of temperature. Particular attention was paid to the region very near the Néel point. The experimental spectra show definite relaxation effects, which are attributed to short-range order with temperature-dependent relaxation times. The soliton model of nonlinear excitations was applied. Experimental data on Fe(III) confirm the predicted exponential temperature dependence of the thermal excitation of moving domain walls.

## Introduction

One of the important recent developments in solid-state physics is the introduction of nonlinear aspects. This soliton concept becomes of growing importance for the study of low-dimensional magnetic systems.<sup>2–5</sup> Solitons in magnetic chains are moving domain walls, which separate spin-up and spin-down regions in a ferromagnet or the two different ordered configurations in an antiferromagnet. These solitons may be conveniently studied in quasi-1-D ionic compounds with easy-axis anisotropy in which the magnetic moments are arranged in widely separated chains such that the ratio of interchain to intrachain exchange interaction  $J'/J$  is very small. These systems allow the construction of a simple picture to describe the physics involved. Since an extensive literature on this subject already exists,<sup>2,7</sup> a review on magnetic solitons will not be undertaken in this paper.

Experimental evidence for this kind of nonlinear excitation has been obtained with techniques such as neutron scattering, nuclear magnetic resonance, and <sup>57</sup>Fe Mössbauer spectroscopy<sup>7</sup>—the last method has been especially useful for high-spin Fe(II) compounds.<sup>8,9</sup> A wall that passes the Mössbauer ion flips the hyperfine field  $H$ , and the flip rate  $W$  may become low enough to fall within the Mössbauer frequency window. For high-spin Fe(II) this frequency range covers many decades, typically from 0.1 to 750 MHz.<sup>8</sup> However, the passage of a soliton at a given site is quite rapid, corresponding to a frequency range of up to  $10^{12}$  s<sup>-1</sup>.<sup>8</sup> For highly ionic Fe(III) fluorides, we expect magnetic hyperfine fields of about 60 T and, therefore, a Mössbauer frequency window of  $0.1\text{--}0.1 \times 10^6$  MHz.

In the following study, we present experimental results obtained by Mössbauer spectroscopy for the quasi-1-D magnetic chain of  $\text{Rb}_2\text{Mn}_{1-x}\text{Fe}_x\text{F}_5\cdot\text{H}_2\text{O}$  ( $x \leq 0.5$ ).<sup>1</sup> We discuss in some detail the dynamic properties of the nonlinear excitations extracted from a series of Fe(III) Mössbauer spectra of the solid solutions.

## Equipment

Magnetic data were obtained from 3 to 300 K by using a vibrating-sample magnetometer in a magnetic field up to 2 T. Mössbauer measurements were performed from 4.2 to 300 K by using a vacuum cryostat. To examine the <sup>57</sup>Fe Mössbauer spectra of the  $\text{Rb}_2\text{Mn}_{1-x}\text{Fe}_x\text{F}_5\cdot\text{H}_2\text{O}$  chains with low Fe content, the <sup>57</sup>Fe isotope was deliberately introduced in small amounts into the compounds. With the aid of a superconducting magnet, a longitudinal external magnetic field was applied to the absorber up to 5 T at a temperature of 4.2 K.

## Preparation and Crystallographic Characterization

Powder samples of  $\text{Rb}_2\text{Mn}_{1-x}\text{Fe}_x\text{F}_5\cdot\text{H}_2\text{O}$  were prepared by the method given in the literature,<sup>10</sup> for which appropriate analytical results are given here. Manganese(III) acetate, iron(III) nitrate, or <sup>57</sup>Fe metal was dissolved in 20% HF, and an aqueous solution of  $\text{Rb}_2\text{CO}_3$  was added. The resulting crystals were removed by filtration, washed with anhydrous methanol, and dried in a vacuum desiccator over KOH. Increasing the amount of  $\text{Rb}_2\text{CO}_3$  resulted in the precipitation of the desired compounds.

The orthorhombic structure of  $\text{Rb}_2\text{MnF}_5\cdot\text{H}_2\text{O}$  (space group *Cmcm*,  $Z = 4$ ) is isostructural with that of  $\text{Rb}_2\text{FeF}_5\cdot\text{H}_2\text{O}$ <sup>10,11</sup> (Figure 1). Iso-

lated infinite, but slightly linked, chains of trans-linked ( $\text{MnF}_6$ ) or ( $\text{FeF}_6$ ) octahedra run along the  $c$  direction. Rubidium atoms and water molecules are located between the chains. The room-temperature lattice parameters of the solid solutions vary continuously between  $x = 0$  and  $x = 0.55$  studied by X-ray crystallography on powder samples (Figure 2). The solid solutions obviously contain in the range  $0.55 < x < 1.0$  a phase mixture of hydrated  $\text{Rb}_2\text{Mn}_{1-x}\text{Fe}_x\text{F}_5\cdot\text{H}_2\text{O}$  and unhydrated  $\text{Rb}_2\text{Mn}_{1-x}\text{Fe}_x\text{F}_5$  compounds corresponding to the trans-linked and cis-linked chain structures, respectively.<sup>11</sup>

A single-crystal study on  $\text{Rb}_2\text{MnF}_5\cdot\text{H}_2\text{O}$  reveals that the complex is tetragonally distorted; the in-plane Mn–F bond lengths are 1.835 and 1.860 Å, and the axial bond lengths are 2.089 Å. The molecular  $z$  axis (of the  $D_{4h}$  molecular unit) is taken parallel to this 2.089-Å bond direction and thus makes an angle of  $4.6^\circ$  with the  $c$  crystallographic axis. The coordination around Mn(III) is very nearly axially symmetric (rhombic distortion is less than 0.2%).<sup>10,12</sup>

The Jahn–Teller theorem is applicable to the degenerate ground state of manganese(III) complexes is octahedral symmetry.<sup>13</sup> In the case of Mn(III) with  $S = 2$  the <sup>5</sup>D term splits in an octahedral field to yield a <sup>5</sup>E<sub>g</sub> ground state and a <sup>5</sup>T<sub>2g</sub> excited state. When the octahedral symmetry of the ligand field is reduced by the Jahn–Teller effect to axial symmetry (the octahedra are remarkably lengthened in the bridging direction<sup>10,12</sup>), the orbital degeneracy of the ground state <sup>5</sup>E<sub>g</sub> is removed.<sup>13</sup> If the  $x$  and  $y$  axes point at the in-plane fluoride atoms, the  $d$  orbitals will be arranged such that  $d_{xz}$ ,  $d_{yz}$  remain degenerate followed by  $d_{xy}$  and  $d_z^2$  and finally by  $d_{x^2-y^2}$  as the most destabilized antibonding orbital. In this scheme, the four 3d electrons will generate a <sup>5</sup>B<sub>1g</sub> ground state.<sup>13</sup> When mixing of the ground and excited states becomes important, the susceptibility values differ for the spin-only prediction and become anisotropic. The zero-field splitting parameter  $D$  characterizes the effect of the spin–orbit interaction and the axially symmetric ligand field in removing the ground-state spin degeneracy of the <sup>5</sup>B<sub>1g</sub> ground term.

The Hamiltonian for the single chain in a magnetic field will have the form<sup>14</sup>

$$H = \sum_i (-2J\vec{S}_i\vec{S}_{i+1} + D(S_{i,x}^2 - \frac{1}{3}S_i(S_i + 1) + E(S_{i,x}^2 - S_{i,y}^2) - g\mu_B\vec{H}\cdot\vec{S}_i) \quad (1)$$

where  $S$  and  $S=(x,y,z)$  are spin operators relating to the actually occupied energy levels. The chain direction is along the  $z$  axis. The first term represents an isotropic Heisenberg exchange interaction between two

- (1) Pebler, J.; Babel, D. *Organic and Inorganic Low-Dimensional Crystalline Materials*; NATO ASI Series, Plenum Press: New York, 1987.
- (2) Bishop, A. R.; Krumhansel, J. A.; Trullinger, S. E. *Physica* **1980**, *D1*, 1.
- (3) Mikeska, R. J. *J. Appl. Phys.* **1981**, *52*, 1950 and references therein.
- (4) Villain, J. *Physica* **1975**, *79B*, 1; In *Ordering in Strongly Fluctuating Condensed Matter Systems*; Riste, Ed.; Plenum Press: New York, 1980; p. 81.
- (5) Maki, K. *Phys. Rev.* **1981**, *214*, 335.
- (6) de Jongh, L. J. *Magneto-Structural Correlations in Exchange Coupled Systems*; NATO ASI Series; D. Reidel: Dordrecht, The Netherlands, 1983.
- (7) de Jongh, L. J. *J. Appl. Phys.* **1982**, *53*, 8018 and references therein.
- (8) de Groot, H. J. M. Thesis, Leiden, The Netherlands, 1986.
- (9) Cheng, C.; Wong, H.; Reiff, W. M. *Inorg. Chem.* **1977**, *16*, 819.
- (10) Bukovec, P.; Kaucic, V. *Acta Crystallogr.* **1978**, *B34*, 3339.
- (11) Fourquet, J. L.; de Pape, R.; Teiller, J.; Varret, F.; Papaefthymiou, G. C. *J. Magn. Magn. Mater.* **1982**, *27*, 209.
- (12) Pebler, J.; Massa, W.; Lass, H.; Ziegler, B. *J. Solid State Chem.* **1987**, *71*, 87.
- (13) Köhler, P.; Massa, W.; Reinen, D.; Hofmann, B.; Hoppe, R. *Z. Anorg. Allg. Chem.* **1978**, *446*, 131.
- (14) Carlin, R. L.; van Duijneveldt, A. J. *Magnetic Properties of Transition Metal Compounds*; Springer-Verlag: New York, 1977.

<sup>†</sup> A preliminary report was given during the NATO Advanced Research Workshop "Organic and Inorganic Low Dimensional Crystalline Materials", May 3–8, 1987, Menorca, Spain.<sup>1</sup>

**Table I.** Concentration Parameter  $x$ , Saturation Fields  $H_{01}$ ,  $H_{02}$ , and  $H_{03}$  at 4.2 K, Iron Contents A1, A2, and A3, and Quadrupole Splittings EQ1, EQ2, and EQ3 at Room Temperature for the Configurations Mn-Fe-Mn, Mn-Fe-Fe, and Fe-Fe-Fe, Respectively, 3-D Ordering Temperature  $T_N$  from Susceptibility Measurements, and Intrachain Exchange Energy  $J_{\text{FeMn}}/k$

$x$	$H_{01}$ , T	$H_{02}$ , T	$H_{03}$ , T	A1, %	A2, %	A3, %	EQ1, mm/s	EQ2, mm/s	EQ3, mm/s	$T_N$ , K	$J_{\text{FeMn}}/k$ , K
0.01	51.1 (3)			100 (2)			0.841 (8)			23.2 (5) <sup>a</sup>	-20.8 (8)
0.10	51.0 (3)	49.2 (3)		93 (2)	7 (3)		0.776 (8)	1.035 (8)		21.0 (1.0)	-19.0 (8)
0.20	50.5 (3)	48.3 (3)		90 (2)	10 (3)		0.788 (8)	1.146 (8)		19.0 (1.0)	-18.7 (8)
0.30	50.2 (3)	48.3 (3)		84 (2)	16 (2)		0.777 (8)	1.127 (6)		17.1 (1.0)	-17.3 (8)
0.40	49.8 (3)	48.3 (3)		70 (2)	30 (2)		0.773 (8)	1.136 (7)		15.5 (5)	-16.0 (8)
0.50	49.3 (3)	47.7 (3)	42.9 (6)	57 (2)	34 (3)	9 (5)	0.786 (8)	1.146 (8)	1.39 (10)	14.5 (5)	-15.3 (8)
1.00 <sup>b</sup>			39.6		100				1.360	9.7	

<sup>a</sup> From neutron diffraction experiments.<sup>19</sup> <sup>b</sup> From ref 11.

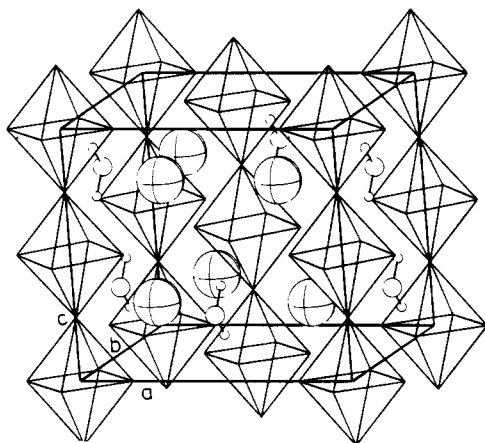


**Figure 1.** Crystal structure of Rb<sub>2</sub>MnF<sub>5</sub>·H<sub>2</sub>O.<sup>10</sup> The space group is assigned to be *Cmcm* ( $Z = 4$ ).

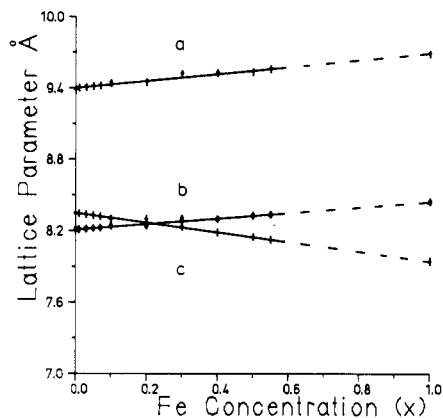


**Figure 2.** Lattice parameters  $a$ ,  $b$ , and  $c$  for Rb<sub>2</sub>Mn<sub>1-x</sub>Fe<sub>x</sub>F<sub>5</sub>·H<sub>2</sub>O ( $x \leq 0.5$ ). The straight lines are guides to the eye. The values for  $x = 1.0$  were taken from ref 11.

neighboring spins on the chain.  $D$  and  $E$  are the axial and rhombic crystal field parameters. The single-ion-type anisotropy may arise from crystal field potential. The rhombic term takes into account the anisotropy in the plane perpendicular to the principal axis. Since it can be shown that  $E \ll D$  and  $J > D$  for all cases of interest here, we distinguish three limiting cases.

$D = 0$ : This isotropic Heisenberg model is characterized by the lack of any preferred direction for the spins. An example is the Fe(III) ion in the high-spin state.

$D > 0$ : This means that the  $z$  axis is a hard axis and the spins lie in a easy plane perpendicular to this axis.

$D < 0$ : In this case, the spins like to point along the easy  $z$  axis. an example is obviously Rb<sub>2</sub>MnF<sub>5</sub>·H<sub>2</sub>O.

Due to the absence of appropriate single-crystals of the title compound for  $x > 0$ , we have recently started to perform studies on proper single crystals of the related solid solution system (NH<sub>4</sub>)<sub>2</sub>Mn<sub>1-x</sub>Fe<sub>x</sub>F<sub>5</sub> in the range between  $x = 0$  and  $x = 0.59$ .<sup>15</sup> Some preliminary results are worth

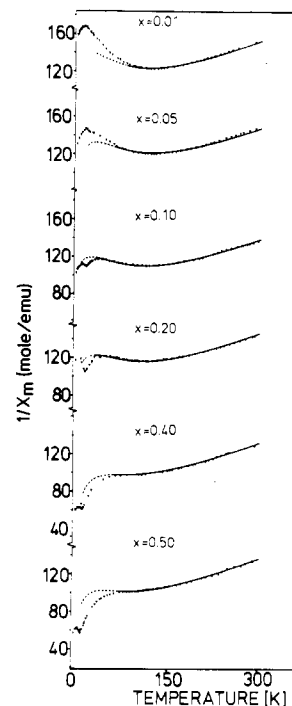


**Figure 3.** Magnetic reciprocal susceptibility  $1/\chi$  of powder samples for Rb<sub>2</sub>Mn<sub>1-x</sub>Fe<sub>x</sub>F<sub>5</sub>·H<sub>2</sub>O compared with theoretical values for a linear isotropic Heisenberg chain (solid curve).<sup>27</sup>

noting. The EPR spectra of (NH<sub>4</sub>)<sub>2</sub>MnF<sub>5</sub> (space group *Pnma*,  $Z = 4$ ) at room temperature are nearly isotropic with two small signals at the  $g$  values  $g_{\perp} = 2.002$  and  $g_{\parallel} = 1.997$ .<sup>16</sup> The high-spin configuration of Mn(III) ( $S = 2$ ) is correlated with an orbital contribution of  $-3 \lambda/\Delta$  for the difference between  $g_{\perp}$  and  $g_{\parallel}$ .<sup>17</sup> With a spin-orbit coupling constant  $\lambda = 70 \text{ cm}^{-1}$ , which is reduced with respect to the free-ion value ( $\lambda_0 = 87 \text{ cm}^{-1}$ ) by 20%, the crystal field splitting may be estimated to be  $\Delta \approx 2.5 \times 10^4 \text{ cm}^{-1}$ . This value is in agreement with the results of ligand field spectroscopy for (NH<sub>4</sub>)<sub>2</sub>MnF<sub>5</sub> reported by Massa et al.<sup>15</sup> Many years ago Kida et al.<sup>17</sup> had determined the intrachain exchange interaction and zero-field splitting (single-ion-type anisotropy) to be  $J = -12.2 \text{ K}$  ( $-8.49 \text{ cm}^{-1}$ ) and  $D = -3.31 \text{ K}$  ( $-2.30 \text{ cm}^{-1}$ ), respectively. They had found that the spins are parallel to the chain axis. This uniaxial spin direction was also confirmed for the Mn(III) and Fe(III) ions in the case of the solid solutions (NH<sub>4</sub>)<sub>2</sub>Mn<sub>1-x</sub>Fe<sub>x</sub>F<sub>5</sub> for  $x = 0.02$ . The exchange and the crystal field parameters were determined to be  $J/k = -12.0$  (5) and  $D/k = -3.2$  (3) K.<sup>18</sup> This determination of the value of the anisotropy constant  $D$  is of critical importance for the evaluation and characterization of the domain wall dynamic, as will be made apparent in the following discussion.

### Results of Investigations

The magnetic susceptibility of Rb<sub>2</sub>Mn<sub>1-x</sub>Fe<sub>x</sub>F<sub>5</sub>·H<sub>2</sub>O was measured from 4.2 to 300 K in external magnetic fields up to 2 T. The observed broad minima in the  $\chi^{-1}$  versus  $T$  curves between

(15) Massa, W.; Pebler, J.; Hahn, F.; Babel, D. *Organic and Inorganic Low-Dimensional Crystalline Materials*; NATO ASI Series; Plenum Press: New York, 1987.

(16) Dance, J. M. Private communication, 1987.

(17) Kida, J.; Watanabe, T. *J. Phys. Soc. Jpn.* **1973**, *34*, 952.

(18) Pebler, J.; Hahn, F.; Massa, W.; Soubeyroux, J. L. To be submitted for publication.

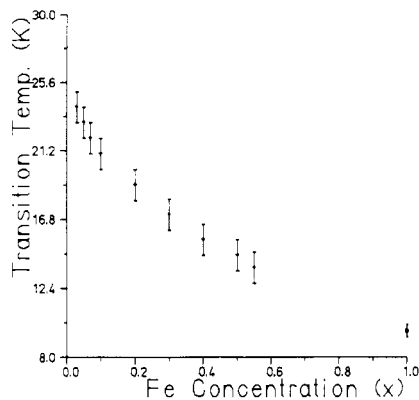


**Figure 4.** Transition temperature  $T_N$  derived from magnetic susceptibility experiments.

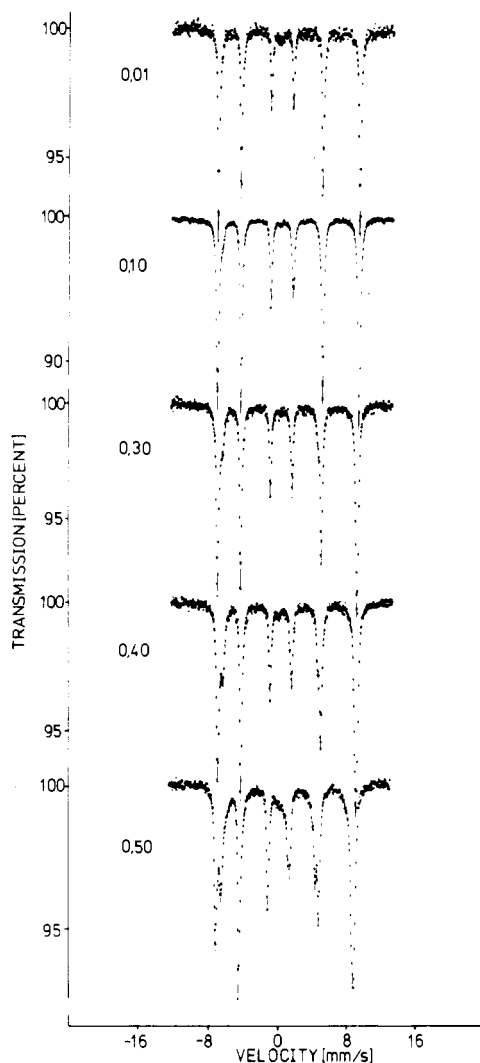


**Figure 5.**  $^{57}\text{Fe}$  Mössbauer spectra of  $\text{Rb}_2\text{Mn}_{1-x}\text{Fe}_x\text{F}_5\cdot\text{H}_2\text{O}$  at 4.2 K.

110 and 130 K were undoubtedly due to short-range antiferromagnetic interaction within the linear chains. With increasing iron concentration, an additional minimum in the reciprocal magnetic susceptibility measured at lower temperatures became sharper. The latter indicated the presence of a 3-D antiferromagnetic order at  $T_N$ , assuming that  $T_N$  is the temperature at which the sharp minimum occurs. We list in Table I these values of  $T_N$  as the 3-D ordering points (see Figure 4). Most recently, these 3-D ordering temperatures were confirmed by neutron diffraction experiments.<sup>19</sup>

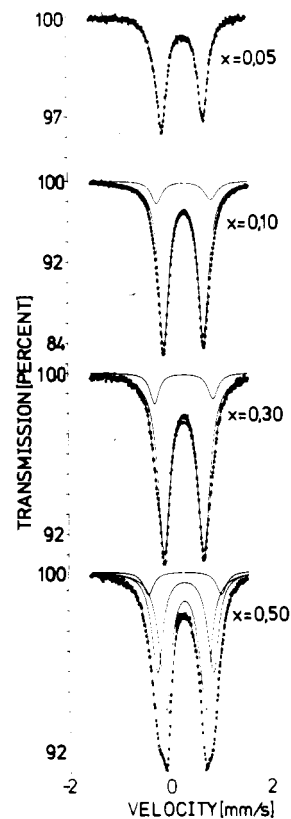


**Figure 6.**  $^{57}\text{Fe}$  Mössbauer spectra of  $\text{Rb}_2\text{Mn}_{1-x}\text{Fe}_x\text{F}_5\cdot\text{H}_2\text{O}$  at room temperature.

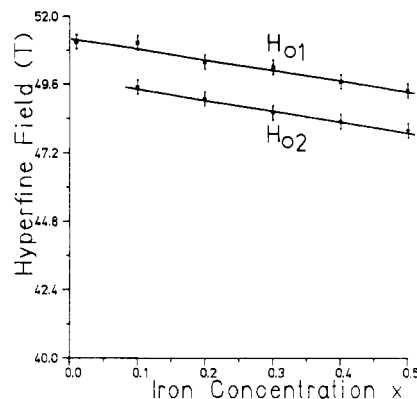


**Figure 7.** Saturation hyperfine fields  $H_{01}$  and  $H_{02}$  at 4.2 K. The straight lines drawn through the data are guides to the eye.

From the results of Mössbauer spectroscopy, we were able to distinguish up to three Fe positions corresponding to the three different (Mn-F-Fe-F-Mn), (Mn-F-Fe-F-Fe), and (Fe-F-Fe-F-Fe) interactions within the random chain and up to three different crystallographically distorted Fe octahedra (see Table I). In Figures 5 and 6 we represent some Mössbauer spectra for samples with different iron concentrations at 4.2 K and room temperature, respectively.

The saturation hyperfine fields  $H_0$  derived at 4.2 K were reduced with increasing iron concentration  $x$  (Table I and Figure 7). In comparison, a saturated value of 39.6 T was reported for  $\text{Rb}_2\text{FeF}_5\cdot\text{H}_2\text{O}$  by Fourquet et al.<sup>11</sup>

Mössbauer spectra for  $x = 0.01$  at 4.2 K under applied magnetic fields up to 5 T showed an antiferromagnetic behavior with an anisotropy energy that was so large that the intensity ratio between the middle and outer lines was field independent from 0 to 5 T within the experimental error (see Figure 8).

The typical values of the chemical shifts and quadrupole splittings, together with the temperature independence of the quadrupole splitting, confirmed the iron atom in the solid solutions to be in the high-spin ferric state (Tables I and II).

(19) Soubeyrou, J. L. Private communication, 1988.

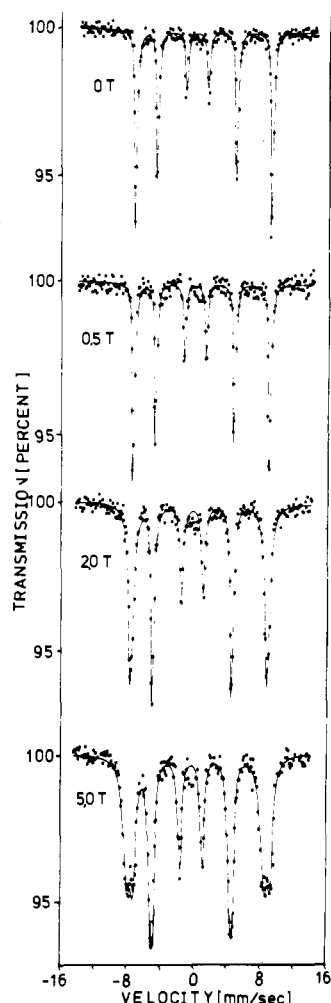


Figure 8. Mössbauer spectra for Rb<sub>2</sub>Mn<sub>1-x</sub>Fe<sub>x</sub>F<sub>5</sub>·H<sub>2</sub>O ( $x = 0.01$ ) at 4.2 K under longitudinal external magnetic fields up to 5 T.

From crystallographic considerations, we assumed, as suggested by Fourquet et al.,<sup>11</sup> that for  $x = 1.0$  the electric field gradient is nearly axial by symmetric along the chain direction. In this case it was the higher energy transition that broadened initially for internal magnetic field fluctuations collinear with  $V_{zz}$ . Therefore, the sign of the quadrupole splitting was positive.<sup>9</sup> To fit the 4.2 K spectra, we assumed that the electric field gradient was not temperature dependent. By using for  $x = 0.01$   $EQ = 0.84$  mm/s and  $\eta \leq 0.3$ , we found that the hyperfine field  $H_0$  should be close to the  $V_{zz}$  gradient axis ( $\phi$  indefinite,  $\theta \approx 0^\circ$ ). This was also confirmed for the  $x = 0.5$  spectrum. In zero magnetic field the iron and presumably the manganese moments were approximately oriented along the chain direction. Since Fe(III) is  $3d^5$ , the single-ion anisotropy of Fe(III) will be negligible. Mn(III) is  $3d^4$  and so should have strong anisotropic properties, which are transmitted via the Mn-Fe exchange to the Fe atoms. The latter become polarized in the same direction as the Mn spins.

Although the easy-axis anisotropy may not be neglected, the temperature dependence of the magnetic susceptibilities was analyzed on the basis of a random classical Heisenberg chain by using the procedure proposed by Fisher<sup>20</sup> for a uniform chain ( $x = 0$ ;  $x = 1.0$ ) and adapted by Thorpe<sup>21</sup> to a random system with two kinds of atoms. Our system provides several situations related to some particular combinations of metal ion sites. The nature of statistical site occupation of metal atoms of different spins gives rise to ferrimagnetic chains. In order to calculate the magnetic susceptibility, we considered the two magnetic species Mn<sup>III</sup> ( $S_{Mn} = 2$ ) and Fe<sup>III</sup> ( $S_{Fe} = 5/2$ ) with concentrations  $1 - x$  and  $x$ , respectively, leading to the three exchange interactions  $J_{MnMn}$ ,

Table II. Mössbauer Parameters for Rb<sub>2</sub>Mn<sub>0.99</sub>Fe<sub>0.01</sub>F<sub>5</sub>·H<sub>2</sub>O Derived from a Fit with a Superposition of Symmetrical Lorentzians<sup>a</sup>

temp, K	magnetic field $H$ , T	isomer shift IS, mm/s	quadrupole splitting EQ, mm/s <sup>b</sup>	line width, mm/s
4.2	51.1 (3)	0.319 (8)	0.850 (8)	0.252 (5)
11.1	50.7 (3)	0.323 (8)	0.838 (8)	0.306 (5)
14.9	50.4 (3)	0.312 (8)	0.848 (8)	0.339 (5)
20.0	48.0 (3)	0.326 (8)	0.836 (8)	0.531 (5)
23.1	46.2 (5)	0.308 (8)	0.834 (10)	0.517 (6)
24.6	43.1 (7)	0.308 (8)	0.844 (12)	1.274 (15)
25.0	38.9 (8)	0.285 (8)	0.792 (15)	1.060 (15)
27.3		0.287 (5)	0.848 (5)	0.315 (5) 0.447 (5)
28.1		0.286 (5)	0.840 (5)	0.309 (5) 0.460 (5)
29.1		0.289 (5)	0.844 (5)	0.280 (5) 0.352 (5)
30.1		0.288 (5)	0.843 (5)	0.263 (5) 0.334 (5)
31.9		0.289 (5)	0.848 (5)	0.253 (5) 0.285 (5)
36.2		0.287 (5)	0.839 (5)	0.246 (5) 0.273 (5)
42.8		0.285 (5)	0.844 (5)	0.240 (5) 0.245 (5)
77.6		0.282 (5)	0.840 (5)	0.239 (5) 0.245 (5)
100.0		0.280 (5)	0.843 (5)	0.237 (5) 0.241 (5)
150.0		0.275 (5)	0.836 (5)	0.253 (5) 0.259 (5)
220.0		0.263 (5)	0.823 (5)	0.249 (5) 0.251 (5)

<sup>a</sup>The isomer shift is given against FeRh. Below 27 K the line widths represent the average of the individual lines. <sup>b</sup> $2\epsilon$  for  $T < T_N \approx 23$  K.

$J_{MnFe} = J_{FeMn}$ , and  $J_{FeFe}$  and therefore to the three  $u$  functions  $u_{MnMn}$ ,  $u_{MnFe} = u_{FeMn}$ , and  $u_{FeFe}$  corresponding to the appropriate pair ions derived in ref 20. The magnetic susceptibility of a random classical Heisenberg linear chain worked out by Thorpe<sup>21</sup> is then given by

$$\chi_m(T) = [N\mu_B^2((xg_1^2 + (1-x)g_2^2)(1-x(1-x)(u_{FeFe}u_{MnMn} - u_{FeMn}^2)) + (xg_1^2 - (1-x)g_2^2)(xu_{FeFe} - (1-x)u_{MnMn}) + 4x(1-x)g_1g_2u_{FeMn})]/[3kT(1-xu_{FeFe} - (1-x)u_{MnMn} + x(1-x)(u_{FeFe}u_{MnMn} - u_{FeMn}^2))] \quad (2)$$

where

$$g_1 = g_{Fe}(S_{Fe}(S_{Fe} + 1))^{1/2}$$

$$g_2 = g_{Mn}(S_{Mn}(S_{Mn} + 1))^{1/2}$$

$$u_{FeFe} = \coth(K_{FeFe} - 1/K_{FeFe})$$

$$K_{FeFe} = 2J_{FeFe}(S_{Fe}(S_{Fe} + 1))$$

$$u_{MnMn} = \coth(K_{MnMn} - 1/K_{MnMn})$$

$$K_{MnMn} = 2J_{MnMn}(S_{Mn}(S_{Mn} + 1))$$

$$u_{FeMn} = \coth(K_{FeMn} - 1/K_{FeMn})$$

$$K_{FeMn} = 2J_{FeMn}(S_{Fe}(S_{Fe} + 1)S_{Mn}(S_{Mn} + 1))^{1/2}$$

The best agreement with the data of the solid solutions obtained by least-squares refinement is given in Figure 3. By fixing  $J_{FeFe}/k = -13.1$  K,<sup>11</sup>  $J_{MnMn}/k = -20.8$  K,<sup>12</sup> and  $g_{Fe} = 2.0$  and varying  $g_{Mn}$  in the range 1.87–2.04, we obtained the interchain exchange energies  $J_{FeMn}/k$  given in Table I. At this level of approximation, the  $g$  factor  $g_{Mn}$  is best regarded as a semiempirical fit parameter. It is worth noting that we have, in addition, calculated the curves by varying  $J_{FeFe}$  and  $J_{MnMn}$  but were unable to obtain more reasonable results.

Clearly, the curves at low Fe concentrations would be brought more nearly into coincidence with the data if anisotropies were taken into account. Finally, it is worth noting that all treatments were based on negligible interchain  $J'$  exchange couplings. This assumption become questionable near the phase transitions  $T_N$  at low temperatures.

The temperature dependence of the Mössbauer spectra for  $x = 0.01$  and  $x = 0.10$  are shown in Figures 9 and 10, respectively. As a first trial, we have analyzed these spectra with symmetric Lorentzian lines. The intensities as well as the line widths were kept as free parameters. For  $x = 0.01$ , the spectra above 42 K were essentially the same. There is some slight temperature-independent asymmetry over this range that we attribute to sample

(20) Fisher, M. E. *Am. J. Phys.* **1964**, *32*, 343.

(21) Thorpe, M. F. *J. Phys.* **1975**, *36*, 1177.

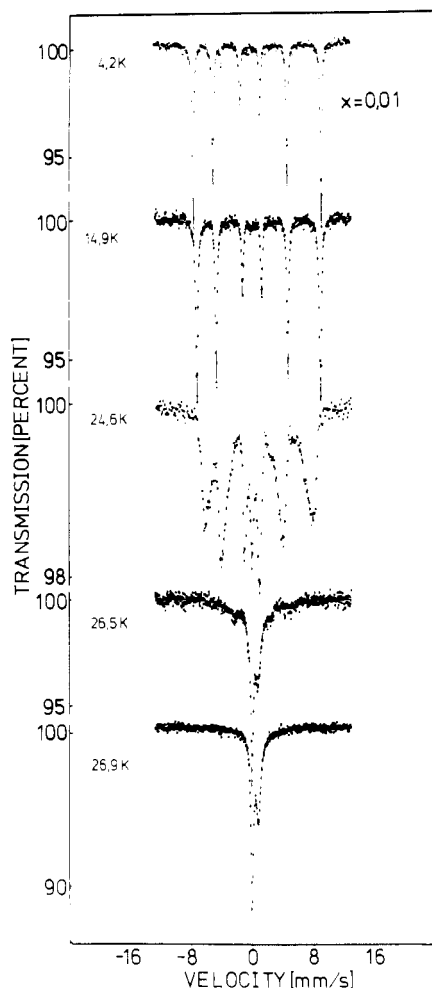


**Figure 9.** Temperature dependence of the Mössbauer spectra for  $\text{Rb}_2\text{Mn}_{1-x}\text{Fe}_x\text{F}_5\cdot\text{H}_2\text{O}$  ( $x = 0.01$ ).

texture. At lower temperatures between 42 and 27 K, an additional temperature-dependent asymmetry of the absorption lines was observed. As the temperature was further decreased, the spectra exhibited magnetic hyperfine splitting corresponding to antiferromagnetic ordering. Somewhere between 27 and 26.5 K the quadrupole doublet of the paramagnetic phase disappeared. The transition to the magnetically split phase was observed by the strong broadening of the lines and by the apparent coexistence of contributions from the paramagnetic and magnetically ordered phase between 23.5 and 27 K. Below 23 K the line widths returned to normal. A pure combined hyperfine pattern was observed that showed an increasing splitting toward lower temperature (see Table II). These important features were common to all other samples studied in the range up to  $x = 0.50$ .

### Discussion

The values of the Néel temperatures in  $\text{Rb}_2\text{Mn}_{1-x}\text{Fe}_x\text{F}_5\cdot\text{H}_2\text{O}$  derived from magnetic susceptibility measurements are low and are consistent with the 1-D character of the solid solutions. The experimental values of the Néel temperatures and, to simplify matters, the calculated intrachain exchange constants  $J_{\text{FeMn}}$  lead to a value of  $R \approx 0.2$  for  $J'/J$ , the ratio of the interchain to intrachain exchange interactions.<sup>22</sup>

In addition to the variation of the magnetic susceptibility, the saturated values  $H_{01}$ ,  $H_{02}$ , and  $H_{03}$  of the hyperfine fields  $H_0$  are evidence in favor of the 1-D character as recently described and reviewed by Johnson.<sup>23</sup> If the saturation value of the hyperfine field for a high-spin  $\text{Fe}^{3+}$  ion is assumed to be 60.0 T ( $H_0 = 61.8$

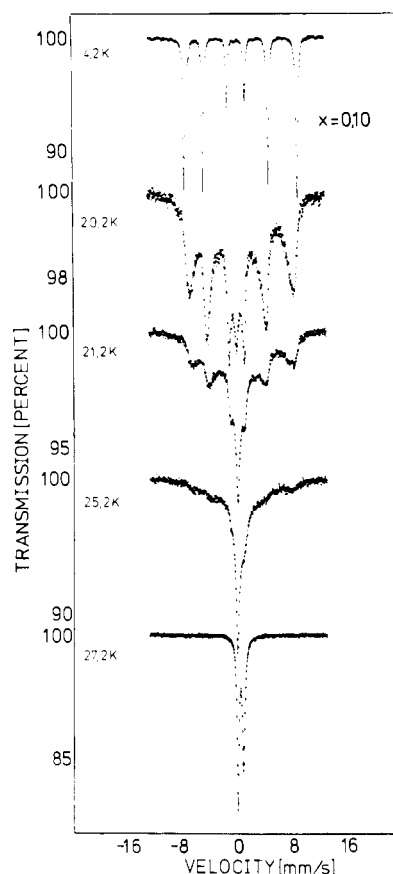


**Figure 10.** Temperature dependence of the Mössbauer spectra for  $\text{Rb}_2\text{Mn}_{1-x}\text{Fe}_x\text{F}_5\cdot\text{H}_2\text{O}$  ( $x = 0.10$ ).

T is observed in the 3-D antiferromagnetically ordered  $\text{FeF}_3$ <sup>24</sup>), the value of  $H_0 = 51.1$  T for  $x = 0.01$  corresponds to a 15% spin reduction.<sup>22,23</sup> It is very unlikely that the value of  $H_0$  is due to covalency effects, in view of the highly ionic nature of the fluorine ligands. We propose that, with decreasing manganese content, the easy-axis anisotropy energy decreases (Figure 7 and Table I).

The paramagnetic quadrupole splittings are remarkably large for a  $^6\text{S}$  state. This might be due to the isolated chain structure and, therefore, to the dipole contribution of the four nonbridging fluorines located in the plane perpendicular to the  $c$  axis. This finding and the positive values of the quadrupole splittings qualitatively show that the octahedra are distorted in such a way that the four fluorine atoms are closer to the iron atom and the two others are more remote as reported in ref 11. The distortion of an individual  $\text{FeF}_6$  octahedron depends on its two neighbors in the chain. Thus, one expects to find three different combinations, viz.,  $\text{Mn}\cdots\text{Fe}\cdots\text{Mn}$ ,  $\text{Mn}\cdots\text{Fe}\cdots\text{Fe}$ , and  $\text{Fe}\cdots\text{Fe}\cdots\text{Fe}$ . Most recently, Massa et al.<sup>15</sup> deduced from ligand field spectra and X-ray crystallographic studies on single crystals of  $(\text{NH}_4)_2\text{Mn}_{1-x}\text{Fe}_x\text{F}_5$  that, in a  $\text{Mn}-\text{F}-\text{Fe}-\text{F}-\text{Fe}$  arrangement, the bridges are more asymmetric than in  $\text{Mn}-\text{F}-\text{Fe}-\text{F}-\text{Mn}$ . A strong  $\text{Fe}-\text{F}$  bond is competing with a weak axial  $\text{Mn}-\text{F}$  bond, which is affected by the Jahn-Teller effect. This may explain the different Fe positions and the difference in the quadrupole splittings listed in Table I.

With increasing iron concentration  $x$ , a decrease in Jahn-Teller distortion along the chain axis is expected. This represents a decrease of the  $\text{Mn}-\text{F}$  distance along the chain as seen by the decrease of the lattice parameter  $c$  in Figure 2 and in ref 15.

Three-dimensional magnetic ordering of the solid solutions studied in the present work is apparent in the low-temperature

(22) Oguchi, T. *Phys. Rev.* **1964**, *133*, A1098.

(23) Johnson, C. E. In *Mössbauer Spectroscopy Applied To Inorganic Chemistry*; Long, G., Ed.; Plenum Press: New York, 1984; Vol. 1.

(24) Wertheim, G. K.; Guggenheim, H. J.; Buchanan, D. N. E. *Phys. Rev.* **1968**, *169*, 465. Pebler, J.; Richter, F. W. Z. *Phys.* **1969**, *221*, 480. Tressaud, A.; Dance, J. M. *Structure and Bonding*; Springer-Verlag: Berlin, 1982; Vol. 52, and references therein.

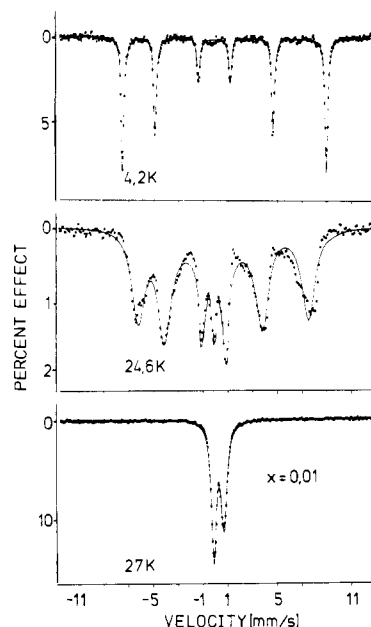


**Figure 11.** Representative Mössbauer spectra for Rb<sub>2</sub>Mn<sub>1-x</sub>Fe<sub>x</sub>F<sub>5</sub>·H<sub>2</sub>O ( $x = 0.01$ ). The continuous line represents a least-squares fit to the applied relaxation model.

magnetically split spectra. Just above and below  $T_N$  we observe an unusual (non-Brillouin) behavior in the temperature dependence of the internal fields. The transition from the paramagnetic state to the magnetically ordered state is accompanied by slow relaxation phenomena. This effect masks the transition usually observed near the critical point and prohibits an accurate determination of the ordering temperature by Mössbauer spectroscopy. The possible occurrence of slow spin-spin relaxation may be excluded, since spin-spin relaxation is obviously fast in magnetically concentrated systems. Additionally, we have considered the occurrence of superparamagnetic effects or spin glass behavior. However, as the magnetically split spectra are still observed above the ordering temperature, this would create a great discrepancy with other experimental results.<sup>25</sup>

Finally, the origin of the broadened asymmetric spectra in the region near the critical point is attributed to residual 1-D correlations above the phase transition. A similar effect is known for the quasi-1-D antiferro- and ferromagnetic Fe<sup>II</sup> chain compounds of the Ising type.<sup>26</sup> The detailed theoretical analysis of domain wall dynamics (solitons, kinks) in magnetic chains by de Jongh and his group<sup>26</sup> shows that, in a certain range above the critical temperature, the density of  $\pi$  domain walls and their motion determine the spin autocorrelation function  $\langle \hat{S}(0)\hat{S}(t) \rangle$ , which is obtained by measuring the fluctuating hyperfine field  $\vec{H}_{hf}(t) \propto \vec{S}(t)$ . In quasi-1-D magnets, the intrachain correlation lengths can be substantial at temperatures  $T \geq 2T_{cr}$ . This explains why magnetic splitting may persist far into the paramagnetic phase.

The Mössbauer spectra below and above the 3-D ordering temperature could successfully be fitted by adopting a relaxation model<sup>27-31</sup> that is appropriate for our Fe<sup>III</sup> system.<sup>32</sup> This takes

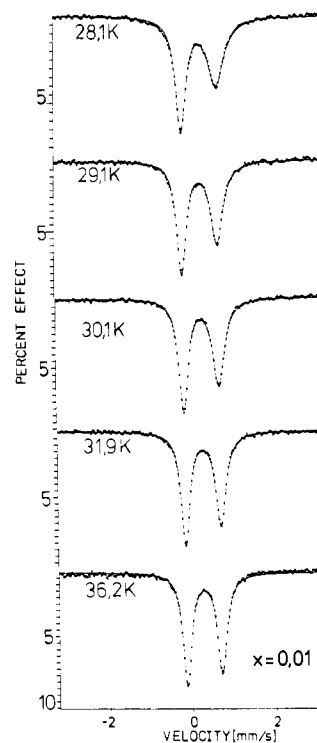


**Figure 12.** Relaxation spectra for Rb<sub>2</sub>Mn<sub>1-x</sub>Fe<sub>x</sub>F<sub>5</sub>·H<sub>2</sub>O ( $x = 0.01$ ) above  $T_N$ .

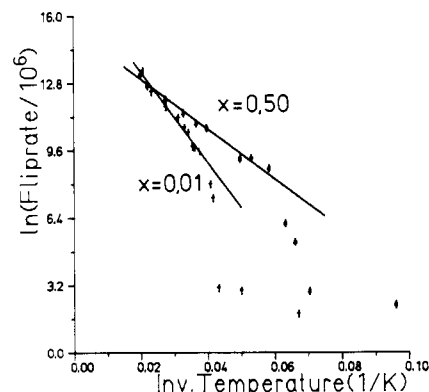


**Figure 13.** Relaxation rate versus inverse temperature for Rb<sub>2</sub>Mn<sub>1-x</sub>Fe<sub>x</sub>F<sub>5</sub>·H<sub>2</sub>O ( $x = 0.01, 0.50$ ). The slopes for the two exponentials are 217 (5) and 124 (5) K.

into account a time-dependent Hamiltonian. Thus, the hf interaction is replaced by a fluctuating effective field, and the decrease in the fluctuation rate causes line broadening, asymmetric spectra, and related phenomena. The line width has been taken to be equal to the low- and high-temperature values of 0.25 mm/s. Below  $T_N$ , the magnetic fields have been taken to be values derived from the fitting procedure of symmetrical Lorentzians (Table II). A gradual decrease of the hyperfine field  $H$  with  $T$  may be understood from the fact that the dynamic is not completely determined by  $\pi$  walls only. For instance, magnon processes will have to be additionally considered. However, at higher temperatures near  $T_N$  where the magnetic hyperfine patterns are not resolved, we are forced to keep constant the values of the magnetic hf fields in the further analysis, e.g. 46.2 and 43.8 T for  $x = 0.01$  and  $x = 0.50$ , respectively. From this approximation, we find the Mössbauer effect to be sensitive to the fluctuations with respect to line broadenings up to  $10^{11}$  s<sup>-1</sup>. Assuming axial symmetry of the electric field gradient tensor along the direction of the magnetic moments, we could fit the spectra<sup>27</sup> by varying the flip rate  $W$  of the hf field  $H$ . From the resolved spectra for  $x = 0.01$ , clusters

- (25) Lass, H.; Pebler, J., In *Industrial Application of the Mössbauer Effect*; Long, G. J., Stevens, J. G., Eds.; Plenum Press: New York, 1986; pp 399-407. Lass, H.; Pebler, J.; Pekala, M.; Polaczek, A. *Phys. Status Solidi A* **1986**, *93*, 233 and references therein.
- (26) de Groot, H. J. M.; Thiel, R. C.; de Jongh, L. J. *Proceedings of an International Workshop*; San Miniato, Italy, 1984; pp 21-26.
- (27) Wickman, H. H.; Wertheim, G. K. Chapter 11 In *Chemical Application of Mössbauer Spectroscopy*; Goldanskii, V.; Herber, R. H., Eds.; Academic Press: New York, 1968; Chapter 11.
- (28) Afanasyev, A. M.; Gorobtschenko, V. D. *Zh. Eksp. Teor. Fiz.* **1974**, *67*, 2246.
- (29) Shenoy, G. K.; Dunlap, B. D. *Proceedings of an International Conference on Mössbauer Spectroscopy*; Cracow, Poland, 1975.
- (30) van der Woude, F.; Decker, A. J. *Phys. Status Solidi* **1966**, *13*, 181.
- (31) Blume, M.; Tjon, J. A. *Phys. Rev.* **1968**, *B165*, 446; **1968**, *B174*, 351.

- (32) Pebler, J. *Phys. Status Solidi A* **1983**, *78*, 589.

with different relaxation frequencies must be present in the temperature range near 24.6 K (Figure 11). At 23.1 K this appears only in asymmetric lines. Between 24 and 26 K, however, there appears in addition—as mentioned above—a central asymmetric double due to faster relaxation that is still observable up to 42 K (see Figures 11 and 12). With equal relaxation rates for the three Fe positions in the compound with  $x = 0.50$ , we can fit the spectra very well. We also analyzed the spectra with different flip rates but were unable to obtain a better agreement with the data.

In Figure 13, we show the spin-flip rate for  $x = 0.01$  and  $x = 0.50$ . The straight lines show the exponential dependence on reciprocal temperature, characteristic for an activated soliton process  $W = \exp(-E_A/kT)$ .<sup>6</sup> The calculated activation energies  $E_A/k$  are 217 (5) and 124 (5) K for  $x = 0.01$  and  $x = 0.50$ , respectively. If the temperature-independent texture effect mentioned above is considered, the activation energy  $E_A/k$  derived from Mössbauer experiments corresponds to 234 (15) K for  $x = 0.01$ . The temperatures at which the drop of the flip rates occurs in Figure 13 correspond to 26.5 and 17.0 K. One may interpret this as a blocking of the domain wall motion by the 3-D long-range order. The 3-D ordering points are a few degrees lower. For  $x = 0.50$ , we determined the value of  $T_N$  to be 14.5 (1.0) K from susceptibility measurements (see Table I).

With decreasing Mn(III) concentration and easy-axis anisotropy energy, the activation energy is reduced by a factor of about 2 for  $x = 0.50$ . This is consistent with the results for  $\text{Rb}_2\text{FeF}_5 \cdot \text{H}_2\text{O}$ . As can be seen from Figure 2b as reported by Fourquet et al.,<sup>11</sup> the spectra above the 3-D phase transition do not display any temperature-dependent line broadening. Solitons are present by virtue of the anisotropy, and for the Fe(III) system, the anisotropy energy will probably be smaller than the 3-D ordering energy  $kT_N$ . The trend of the activation energy obtained from the Mössbauer experiments is so far quite convincing. Such a decrease of the

activation energy with decreasing anisotropy energy may be understood from the classical domain wall theory (for review see ref 8)

$$E_s = 2\pi S^2(D \cdot J)^{1/2} \quad (3)$$

where  $E_s$  represents the creation energy of solitons. This approximation may be convenient if the spin value is large, so that the classical spin vector is approached, and if the characteristic wavelengths of the fluctuations in the spin system (e.g. the widths of the solitons) are large compared to the lattice spacing. Assuming that the classical domain wall theory is also valid in our case of a random system and inserting in eq 3 the experimental values of  $J_{\text{FeMn}}$  (as an averaged value of  $J$ ),  $E_s = E_A$  and the average spin of the solid solutions, we can estimate the anisotropy constants  $D = E_A^2/(4\pi^2 S^4 J)$  to be equal to 3.0 (3) and 1.0 (3) K for  $x = 0.01$  and  $x = 0.50$ , respectively. The value of the anisotropy constant for  $x = 0.01$  is in fair agreement with the  $D$  values derived from magnetic susceptibility measurements on single crystals of the related solid solutions  $(\text{NH}_4)_2\text{Mn}_{1-x}\text{Fe}_x\text{F}_5$  with  $x = 0$  and  $x = 0.02$ <sup>17,18</sup> mentioned above. The preliminary results on  $(\text{NH}_4)_2\text{Mn}_{0.55}\text{Fe}_{0.45}\text{F}_5$  seem to confirm such a decrease of  $D$  with increasing Fe content. Unfortunately, however, the magnetic structure, apparently important for establishing this correlation, is more complex than those derived for the lowest  $x$  values. Therefore, a Mössbauer and neutron diffraction study on powder samples and a study of the magnetic susceptibility on single crystals of  $(\text{NH}_4)_2\text{Mn}_{1-x}\text{Fe}_x\text{F}_5$  up to  $x = 0.60$  are now under investigation.<sup>18</sup>

**Acknowledgment.** I am indebted to J. L. Soubeyroux (ILL, Grenoble, France) for the neutron diffraction experiment. I am also indebted to J. M. Dance for the  $g$  factor measurement. The financial support of the Commission of the European Community is gratefully acknowledged.

Contribution from the Fachbereich Chemie der Philipps-Universität, D-3550 Marburg/Lahn, FRG

## Color and Electronic Structure of Manganese(V) and Manganese(VI) in Tetrahedral Oxo Coordination. A Spectroscopic Investigation

Herbert Lachwa and Dirk Reinen\*

Received July 29, 1988

From the single-crystal EPR spectra of Mn(V) in tetrahedral oxo coordination in the compounds  $\text{Ca}_2(\text{MO}_4)\text{Cl}$  [ $M = \text{P(V)}, \text{V(V)}, \text{As(V)}$ ] with the spodosite structure are derived the ground-state electronic structure and the geometry and orientation of the  $\text{MnO}_4$  polyhedra in the host lattice, and the obtained zero-field-splitting parameters are compared with those from powder EPR spectra of various other oxo compounds. In the case of  $M = \text{P(V)}$ , where a considerable mismatch between the volume of the doped and the host polyhedra exists, the  $\text{MnO}_4^{3-}$  entities are flattened to a greater extent than the  $\text{PO}_4^{3-}$  tetrahedra and also the axis of compression has a slightly different orientation. The reflectance spectra are assigned with respect to the d-d and charge-transfer transitions on the basis of literature data and related to the color properties. The correlation of the color shift from green to blue of the prepared Mn(V) compounds with the host site geometry, the chemical constitution, and the Mn(V) concentration is discussed. Finally, a comparison with corresponding spectral data for Mn(VI) is made.

### Introduction

Intensive and bright colors are observed if transition-metal ions are incorporated into the tetrahedral sites of solid host compounds. Manganese(V) can be stabilized in tetraoxo coordination by isomorphous substitution in phosphate compounds and induces blue or green colors.<sup>1-4</sup> Recently, the first single-crystal X-ray structure investigation of a Mn(V) compound, namely  $\text{Ba}_5(\text{MnO}_4)_3\text{Cl}$ , which crystallizes in the apatite structure, was performed.<sup>4</sup> The stability of Mn(V) is strongly dependent on the simultaneous

presence of cations with pronounced base properties. The mixed crystals  $\text{A}^{II}_5(\text{PO}_4)_{3-x}(\text{MnO}_4)_x\text{X}$  ( $X = \text{Cl}^-, \text{OH}^-, \text{F}^-$ ) can be synthesized over the whole range of  $x$  values for  $\text{A}^{II} = \text{Ba}^{2+}$ , with color variations from light blue at very low Mn(V) concentrations through turquoise-blue and green to dark green for  $x = 3$  (Figure 1). The corresponding compounds with  $\text{Sr}^{2+}$  and  $\text{Ca}^{2+}$  are only stable up to  $x = 1.5$  and  $x = 0.1$ , respectively, and are blue at low doping concentrations.<sup>4</sup> Single-crystal electronic spectra of tetrahedral Mn(V) in host lattices with the apatite and spodosite structure and band assignments are reported by Day et al.<sup>5</sup> and Milstein and Holt.<sup>6</sup> Electronic reflection and powder EPR data, which were analyzed with respect to the zero-field splitting pa-

(1) Lux, H. Z. *Naturforsch.* **1946**, *1*, 281.

(2) Klemm, W. *Angew. Chem.* **1954**, *66*, 468. Krause, J. Dissertation, University of Münster, 1954.

(3) Scholder, R. *Angew. Chem.* **1954**, *66*, 461.

(4) Reinen, D.; Lachwa, H.; Allmann, R. Z. *Anorg. Allg. Chem.* **1986**, *542*, 71.

(5) Borromei, R.; Oleari, L.; Day, P. J. *Chem. Soc., Faraday Trans.* **1977**, *73*, 135; **1981**, *77*, 1563.

(6) Milstein, J.; Holt, S. L. *Inorg. Chem.* **1969**, *8*, 1021.